Field-induced SIM behaviour of Co(II) complex with 1,1'-diacetylferrocene-derived ligand

Yulia P. Tupolova,[a] Igor N .Shcherbakov,*[a] Leonid D. Popov,[a] Roman B. Morgunov,[b] Denis V. Korchagin,[b] Vladimir E. Lebedev,[a] Andrei V. Palii,[b,c] Sergey M. Aldoshin

[a] Department of Chemistry, Southern Federal University, 7, Zorge Str., Rostov-on-Don, 344090, Russia

[b] Institute of Problems of Chemical Physics of the Russian Academy of Sciences, Chernogolovka, Moscow Region, Russia

[c] Institute of Applied Physics, 5, Academiei str. Chisinau, MD-2028 Moldova

Electronic Supplementary Information

X_Ray single crystal diffraction study of I. X-ray data for a single crystal of **I** were collected on a CCD diffractometer Agilent XCalibur with EOS detector (Agilent Technologies UK Ltd, Yarnton, Oxfordshire, England) using graphite-monochromated MoK_α radiation (λ= 0.71073 Å) and treated by CrysAlisPro software for cell refinement, data collection, and data reduction with empirical absorption correction (Scale3AbsPack) of the experimental intensities [1]. The structure was solved by direct methods and refined against all F^2 data [2]. All non-hydrogen atoms were refined with anisotropic thermal parameters, positions of hydrogen atoms were obtained from difference Fourier syntheses and refined with riding model constraints. The X-ray crystal structure data have been deposited with the Cambridge Crystallographic Data Center, with reference codes CCDC 2020491. Selected crystallographic parameters and the data collection and refinement statistics are given in Table S1, ESI†, selected bond lengths and angles are presented in Tabl2 S2, ESI†. The powder XRD measurements show that sample of compound **I** is the monophase crystalline material (Fig. S1.).

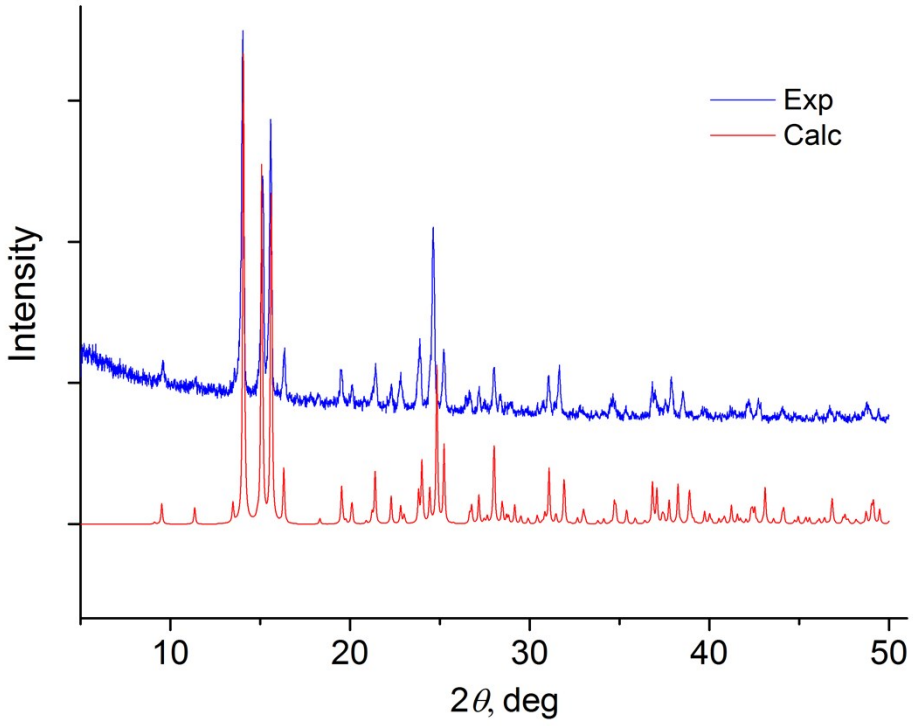

Figure S1. Powder X-ray diffraction pattern of polycrystalline samples of complexes: experimental for complex **I** (blue) and calculated from single crystal data for complex **I** (red).

Table S1. Crystal data and structure refinement for **I**

Parameters	**Values**
formula (M)	$C_{26}H_{24}Cl_2Co_1Fe_1N_6O_{0.09}$ (607.63)
Temperature, K	100.0(1)
crystal system, space group	tetragonal, $P4_12_12$
a=b, Å	13.1248(2)
c, Å	14.3338(2)
Volume, Å^3	2469.15(8)
Z, ρ_{calc}, g/cm^3	4, 1.635
μ, mm^{-1}	1.505
F(000)	1239
Crystal size, mm^3	0.35×0.15×0.15
θ range, °	3.10 - 29.05
Index ranges	$-13 \le h \le 17$, $-17 \le k \le 12$, $-17 \le l \le 19$
Reflections collected / unique [R(int)]/ I>2σ(I)	9188 / 3260 [0.0265] /
Completeness to θ	0.998
Number of parameters	171
GOOF	1.061
Final R indices [I>2σ(I)]	$R_1 = 0.0258$, $wR_2 = 0.0598$
R indices (all data)	$R_1 = 0.0298$, $wR_2 = 0.0624$
Absolute structure parameter	-0.024(12)
$\Delta\rho_{max}$ / $\Delta\rho_{min}$, e·Å^{-3}	0.482 / -0.341

Table S2. Selected bond lengths [Å] and angles [deg] for compound **I**.

Bond	**d, Å**	**Bond**	**d, Å**
Co(1)-N(1)	2.161(2)	Co(1)-N(2)	2.203(2)
Co(1)-Cl(1)	2.4429(5)	Fe(1)-C(3)	2.036(2)
Fe(1)-C(4)	2.039(2)	Fe(1)-C(5)	2.039(2)
Fe(1)-C(1)	2.056(2)	Fe(1)-C(2)	2.052(2)
N(1)-C(10)	1.343(3)	N(1)-C(6)	1.358(3)
N(2)-C(11)	1.289(3)	N(3)-C(12)	1.287(3)
N(2)-N(3)	1.403(3)	C(12)-C(4)	1.469(3)
C(7)-C(6)	1.389(3)	C(7)-C(8)	1.391(3)
C(9)-C(8)	1.388(3)	C(9)-C(10)	1.388(3)
C(6)-C(11)	1.455(3)	C(12)-C(13)	1.503(3)
C(1)-C(2)	1.421(3)	C(1)-C(5)	1.424(3)
C(4)-C(3)	1.440(3)	C(4)-C(5)	1.442(3)
C(2)-C(3)	1.418(3)		
Angle	**ω,°**	**Angle**	**ω,°**
N(1)-Co(1)-N(1)$^{\#1}$	109.44(9)	C(3)-Fe(1)-C(4)$^{\#1}$	111.98(9)
N(1)-Co(1)-N(2)$^{\#1}$	172.63(7)	C(5)-Fe(1)-C(4)$^{\#1}$	132.47(9)
Cl(1)-Co(1)-Cl(1)$^{\#1}$	168.82(3)	C(4)-Fe(1)-C(2)$^{\#1}$	143.96(9)
N(1)-Co(1)-N(2)	76.19(6)	C(3)$^{\#1}$-Fe(1)-C(2)	174.59(9)
N(2)$^{\#1}$-Co(1)-N(2)	98.63(9)	C(3)-Fe(1)-C(2)	40.58(9)
N(1)-Co(1)-Cl(1)	82.66(5)	C(5)-Fe(1)-C(2)	68.60(9)
N(1)$^{\#1}$-Co(1)-Cl(1)	90.87(5)	C(5)$^{\#1}$-Fe(1)-C(2)	114.31(9)
N(2)$^{\#1}$-Co(1)-Cl(1)	92.64(5)	C(4)$^{\#1}$-Fe(1)-C(2)	143.96(9)
N(2)-Co(1)-Cl(1)	94.65(5)	C(4)-Fe(1)-C(2)	68.91(9)
C(10)-N(1)-Co(1)	128.25(15)	C(2)$^{\#1}$-Fe(1)-C(2)	135.92(13)
C(6)-N(1)-Co(1)	114.13(13)	C(3)$^{\#1}$-Fe(1)-C(1)	134.38(9)
C(11)-N(2)-N(3)	114.02(18)	C(3)-Fe(1)-C(1)	68.53(9)
C(11)-N(2)-Co(1)	113.80(14)	C(5)-Fe(1)-C(1)	40.71(9)
N(3)-N(2)-Co(1)	131.31(13)	C(5)$^{\#1}$-Fe(1)-C(1)	145.50(9)
N(1)-C(6)-C(11)	116.42(18)	C(4)$^{\#1}$-Fe(1)-C(1)	173.03(9)
C(2)-C(1)-C(5)	108.3(2)	C(3)$^{\#1}$-Fe(1)-C(3)	143.34(13)
C(4)-C(12)-C(13)	119.05(19)	C(3)$^{\#1}$-Fe(1)-C(5)	108.30(9)
N(3)-C(12)-C(4)	115.72(19)	C(3)-Fe(1)-C(5)	69.32(9)

C(8)-C(9)-C(10)	118.8(2)	C(4)-Fe(1)-C(1)	68.97(9)
C(6)-C(7)-C(8)	119.0(2)	C(2)$^{\#1}$-Fe(1)-C(1)	111.29(9)
N(3)-C(12)-C(13)	125.2(2)	C(2)-Fe(1)-C(1)	40.46(9)
C(3)-Fe(1)-C(5)$^{\#1}$	108.29(9)	C(3)-Fe(1)-C(1)$^{\#1}$	134.38(9)
C(5)-Fe(1)-C(5)$^{\#1}$	172.85(13)	C(5)-Fe(1)-C(1)$^{\#1}$	145.50(9)
C(3)$^{\#1}$-Fe(1)-C(4)	111.98(9)	C(4)-Fe(1)-C(1)$^{\#1}$	173.03(9)
C(4)$^{\#1}$-Fe(1)-C(4)	106.55(12)	C(2)-Fe(1)-C(1)$^{\#1}$	111.29(9)
C(3)-Fe(1)-C(4)	41.38(8)	C(1)-Fe(1)-C(1)$^{\#1}$	115.99(13)
C(5)-Fe(1)-C(4)	41.43(9)	C(10)-N(1)-C(6)	117.25(19)
C(5)$^{\#1}$-Fe(1)-C(4)	132.47(9)	C(12)-N(3)-N(2)	117.05(18)
C(3)-Fe(1)-C(2)$^{\#1}$	174.59(9)	C(2)-C(1)-Fe(1)	69.62(13)
C(5)-Fe(1)-C(2)$^{\#1}$	114.31(9)	C(5)-C(1)-Fe(1)	69.00(12)
C(7)-C(6)-C(11)	120.9(2)	C(4)-C(3)-Fe(1)	69.42(12)
N(1)-C(10)-C(9)	123.5(2)	C(1)-C(5)-C(4)	107.97(19)
N(2)-C(11)-C(6)	119.2(2)	C(1)-C(5)-Fe(1)	70.29(13)
C(9)-C(8)-C(7)	118.7(2)	C(4)-C(5)-Fe(1)	69.29(12)
C(3)-C(2)-C(1)	108.5(2)	C(3)-C(4)-C(5)	107.05(19)
C(3)-C(2)-Fe(1)	69.11(13)	C(3)-C(4)-C(12)	126.17(19)
C(1)-C(2)-Fe(1)	69.91(12)	C(5)-C(4)-C(12)	126.74(19)
C(2)-C(3)-C(4)	108.2(2)	C(3)-C(4)-Fe(1)	69.20(12)
C(2)-C(3)-Fe(1)	70.32(13)	C(5)-C(4)-Fe(1)	69.28(12)
N(1)-C(6)-C(7)	122.73(19)	C(12)-C(4)-Fe(1)	124.78(15)

Symmetry transformations used to generate equivalent atoms: $^{\#1}$ y, x, -z

Computational details

Theoretical calculations of the electronic structure for complex **I** were performed using a post-Hartree–Fock multi-reference wavefunction (WF) approach based on state-averaged complete active space self-consistent field calculations (SA-CASSCF) [3-5] followed by N-electron valence second-order perturbation theory (NEVPT2) [6-9]. Scalar relativistic effects were account for using a standard second-order Douglas–Kroll–Hess (DKH) procedure [10]. For calculations, a segmented all-electron relativistically contracted version [11] of Ahlrichs polarized triple-zeta basis set, def2-TZVP [12-14], was used for all atoms. To improve the

calculation time, the resolution of the identity approximation with corresponding correlation fitting of the basis set [15] was employed. Spin–orbit effects were included using the quasi-degenerate perturbation theory (QDPT) [16].

The CASSCF active space was constructed from 5 MOs with predominant contributions of 3d-AOs from the metal center and 7 electrons, corresponding to metal ion CAS(7, 5). Ten quartets and 40 doublet states were included in the WF expansion.

For all calculations, nuclei coordinates of non-hydrogen atoms were taken from diffraction experimental data, and positions of hydrogen atoms were optimized employing density functional theory with the BP86 functional and Ahlrichs polarized basis set def2-TZVP (optimized nuclei coordinates are listed in Table S3, ESI†).

Splitting of the d-orbitals was analyzed within the *ab initio* ligand field theory (AILFT) [17, 18] as implemented in ORCA software.

Table S3. Atomic coordinates used for ZFS calculations (hydrogen atoms positions optimized at BP86/def2-TZVP level of theory while non-hydrogen atoms are fixed at positions obtained from single crystal X-ray diffraction study)

Co	1.18971914813404	2.43824272001278	3.84869710627750
Cl	-0.18186259214886	4.12032682083468	4.87545033051699
Cl	1.70312603817490	1.26161553675098	1.91678473236533
N	1.37317279635709	1.08766976188048	5.55623357669205
N	0.38913896411349	0.19057695262195	5.80699390632533
H	0.43478349364151	-0.51209342526760	6.54313480126880
N	-0.68055087277282	1.06532175307572	3.94447962065723
N	-1.56420952826155	-0.80589356092489	5.18239033099433
N	3.06463116477177	2.82456176766218	4.84034618643296
N	3.87067086616076	3.80531768789111	4.36719120526593
H	4.77262137208214	4.04039543629593	4.77742010583841
N	4.26256515019149	5.50011373367696	2.91056151909313
N	2.20865441834349	4.25301259632579	2.81373561504133
C	2.43947701097685	1.12329712545256	6.29433060448735
C	2.72670228634025	0.20499507096314	7.44068740399518

H	2.41970090343034	-0.82863481945039	7.20790531570810
H	2.18891067241559	0.50406453885503	8.35702597872827
H	3.79344698813122	0.16410767769881	7.67743115233871
C	-0.66778378417222	0.15769447247272	4.92581307535958
C	-1.74498699609382	0.99348631268115	3.11115001411065
C	-2.72398558207923	0.03839574909009	3.28848089523873
H	-3.57450919880330	-0.00342684911136	2.60728037582524
C	-2.61970349195841	-0.84950357400545	4.34197351914159
C	-1.80435316554295	1.97173132518225	1.98475525656382
H	-1.77890301839432	2.99609505272922	2.38491459635777
H	-2.71269016097494	1.83496979081578	1.38526128894037
H	-0.91360614862493	1.84540534805283	1.35048521668649
C	-3.66027215437701	-1.89663921947313	4.60698515221548
H	-3.19463878349035	-2.89016165574136	4.67680652305440
H	-4.42656626539648	-1.91335407757991	3.82153651219807
H	-4.15288993113895	-1.70736197486248	5.57323684614464
C	3.40220793594393	2.16831765791826	5.89469905576965
C	4.63664002973317	2.44344348328765	6.69427589449769
H	5.55218758871295	2.11862626366369	6.16870636313834
H	4.62043766291059	1.94641987065127	7.66705338182412
H	4.74096926099399	3.52362835572344	6.89339771609101
C	3.42101289719801	4.54887626252242	3.30120918712917
C	3.83934040012566	6.26958446917665	1.89236168009109
C	2.60132002031852	6.05327420353336	1.29829450340347
H	2.25492989980073	6.67741564366265	0.47521096957315
C	1.79671444547130	5.02929565848039	1.78783944106740
C	0.44372933711223	4.74673187569154	1.22892002039638
H	-0.29584050311531	4.79748824927277	2.04347755958245
H	0.41954255430901	3.72253898940412	0.82772878820242
H	0.17643789212494	5.45763845335371	0.43801324288670
C	4.77112355671134	7.35134349797880	1.44797253143042
H	5.73406457093274	6.91959402910271	1.13778872234600
H	4.98500502193132	8.03614829278198	2.28223927987638
H	4.35730982975006	7.92963666918903	0.61256789883039

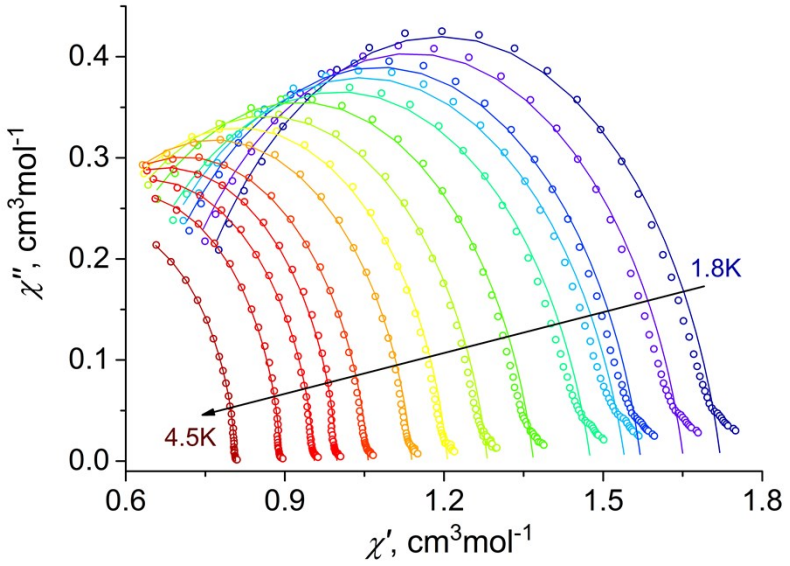

Figure S2. Cole-Cole diagrams for **I** at H_{DC} = 1000 *Oe* (points – experiment, lines – fit by generalized Debye model).

Table S4. Best fit parameters of the generalized Debye model for the Cole-Cole plot of complex **I** at H_{DC} =1000 Oe

T, K	χ_S, cm^3 mol^{-1}	χ_T, cm^3 mol^{-1}	τ, s	α	R_1 [a]
1.8	0.666	1.722	5.76E-04	0.145	1.1E-02
1.9	0.623	1.652	5.15E-04	0.153	1.1E-02
2.0	0.584	1.571	4.57E-04	0.149	0.9E-03
2.1	0.548	1.541	4.10E-04	0.169	1.2E-02
2.2	0.528	1.476	3.80E-04	0.164	9.2E-03
2.4	0.483	1.369	3.09E-04	0.139	5.3E-03
2.6	0.447	1.282	2.57E-04	0.127	3.8E-03
2.8	0.419	1.207	2.18E-04	0.112	2.4E-03
3.0	0.392	1.139	1.85E-04	0.102	1.5E-03
3.3	0.362	1.057	1.46E-04	0.091	1.0E-03
3.5	0.356	0.998	1.31E-04	0.064	6.8E-04
3.7	0.331	0.956	1.10E-04	0.073	4.7E-04
4.0	0.324	0.892	0.95E-04	0.045	2.6E-04
4.5	0.301	0.807	0.70E-04	0.047	7.1E-05

[a] The mean residual sum of squares, $R_1 = \frac{1}{n}\sum_{i=1}^{n}\frac{(Y_{\text{exp}} - Y_{\text{calc}})^2}{Y_{\text{exp}}^{\ 2}}$

Table S5. Spin-free state (δ_E) and spin-orbit state (Δ_E) energies (cm^{-1}) calculated with CASSCF and CASSCF+NEVPT2 approximations.

	CASSCF		CASSCF+NEVPT2	
Spin	Spin-free states (δ_E)	Spin-orbit states (Δ_E)	Spin-free states (δ_E)	Spin-orbit states (Δ_E)
3/2	0.0	0.0 99.1	0.0	0.0 77.6
3/2	1055.6	1123.7 1299.4	1407.6	1464.8 1588.4
3/2	1640.9	1896.3 1947.3	2277.4	2467.5 2507.4
3/2	5774.2	5969.4 6043.0	7994.0	8131.2 8188.4

References

[1] Agilent (2011). CrysAlis PRO version 171.35.19, Agilent Technologies UK Ltd, Yarnton, Oxfordshire, England, in, 2011.
[2] G.M. Sheldrick, G.M. Sheldrick (8/06/2000). SHELXTL v. 6.14, Structure Determination Software Suite, Bruker AXS, Madison, Wisconsin, USA, in, 2000.
[3] B.O. Roos, P.R. Taylor, P.E.M. Sigbahn, A complete active space SCF method (CASSCF) using a density matrix formulated super-CI approach, Chem. Phys., 48 (1980) 157-173.
[4] S. Per, H. Anders, R. Björn, L. Bernard, A Comparison of the Super-CI and the Newton-Raphson Scheme in the Complete Active Space SCF Method, Phys. Scr., 21 (1980) 323.
[5] P.E.M. Siegbahn, J. Almlöf, A. Heiberg, B.O. Roos, The complete active space SCF (CASSCF) method in a Newton–Raphson formulation with application to the HNO molecule, J. Chem. Phys., 74 (1981) 2384-2396.
[6] C. Angeli, R. Cimiraglia, S. Evangelisti, T. Leininger, J.P. Malrieu, Introduction of n-electron valence states for multireference perturbation theory, J. Chem. Phys., 114 (2001) 10252-10264.
[7] C. Angeli, R. Cimiraglia, J.-P. Malrieu, N-electron valence state perturbation theory: a fast implementation of the strongly contracted variant, Chem. Phys. Lett., 350 (2001) 297-305.
[8] C. Angeli, R. Cimiraglia, Multireference perturbation configuration interaction V. Third-order energy contributions in the Møller–Plesset and Epstein–Nesbet partitions, Theor. Chem. Acc., 107 (2002) 313-317.
[9] C. Angeli, R. Cimiraglia, J.-P. Malrieu, n-electron valence state perturbation theory: A spinless formulation and an efficient implementation of the strongly contracted and of the partially contracted variants, J. Chem. Phys., 117 (2002) 9138-9153.
[10] B.A. Hess, Relativistic electronic-structure calculations employing a two-component no-pair formalism with external-field projection operators, Phys. Rev. A, 33 (1986) 3742-3748.
[11] D.A. Pantazis, X.Y. Chen, C.R. Landis, F. Neese, All-electron scalar relativistic basis sets for third-row transition metal atoms, J. Chem. Theory Comput., 4 (2008) 908.
[12] A. Schafer, C. Huber, R. Ahlrichs, Fully optimized contracted Gaussian basis sets of triple zeta valence quality for atoms Li to Kr, J. Chem. Phys., 100 (1994) 5829-5835.

[13] A. Schafer, H. Horn, R. Ahlrichs, Fully optimized contracted Gaussian basis sets for atoms Li to Kr, J. Chem. Phys., 97 (1992) 2571-2577.
[14] F. Weigend, R. Ahlrichs, Balanced basis sets of split valence, triple zeta valence and quadruple zeta valence quality for H to Rn: Design and assessment of accuracy, Physical Chemistry Chemical Physics, 7 (2005) 3297-3305.
[15] F. Neese, An improvement of the resolution of the identity approximation for the formation of the Coulomb matrix, J. Comput. Chem., 24 (2003) 1740-1747.
[16] D. Ganyushin, F. Neese, First-principles calculations of zero-field splitting parameters, J. Chem. Phys., 125 (2006) 024103.
[17] M. Atanasov, D. Ganyushin, K. Sivalingam, F. Neese, in: D.M.P. Mingos, P. Day, J.P. Dahl (Eds.) Molecular Electronic Structures of Transition Metal Complexes II, Springer Berlin Heidelberg, Berlin, Heidelberg, 2012, pp. 149-220.
[18] S.K. Singh, J. Eng, M. Atanasov, F. Neese, Covalency and chemical bonding in transition metal complexes: An ab initio based ligand field perspective, Coord. Chem. Rev., 344 (2017) 2-25.